Exploring new strategies for ozone-risk assessment: a dynamic-threshold case study

[1]Conte A., [2]Otu-Larbi F., [1]Alivernini A., [3]Hoshika Y., [3]Paoletti E., [2]Ashworth K., [1,4]Fares S.*

[1] *Council for Agricultural Research and Economics (CREA), Research Centre for Forestry and Wood (FL), Rome 00166, Italy*

[2] *Lancaster Environment Centre, Lancaster University, Lancaster LA1 4YQ, UK.*

[3] *National Research Council of Italy (CNR), Institute of Research on Terrestrial Ecosystems (IRET), Sesto Fiorentino 50019, Italy*

[4] *National Research Council of Italy (CNR), Institute of BioEconomy (IBE), Rome 00185, Italy*

**Corresponding author: silvano.fares@cnr.it*

Abstract

Tropospheric ozone is a dangerous atmospheric pollutant for forest ecosystems when it penetrates stomata. Thresholds for ozone-risk assessment are based on accumulated stomatal ozone fluxes such as the Phytotoxic Ozone Dose (POD). In order to identify the effect of ozone on a Holm oak forest in central Italy, four flux-based ozone impact response functions were implemented and tested in a multi-layer canopy model AIRTREE and evaluated against Gross Primary Productivity (GPP) obtained from observations of Eddy Covariance fluxes of CO_2. To evaluate if a clear phytotoxic threshold exists and if it changes during the year, six different detoxifying thresholds ranging between 0 and 5 nmol O_3 m^{-2} s^{-1} were tested.

The use of species-specific rather than more general response functions based on plant functional types (PFT) increased model accuracy (RMSE reduced by up to 8.5%). In the case of linear response functions, a threshold of 1 nmol m^{-2} s^{-2} produced the best results for simulations of the whole year, although the tolerance to ozone changed seasonally, with higher tolerance (5 nmol m^{-2} s^{-1} or no ozone impact) for Winter and Spring and lower thresholds in Summer and Fall (0-1 nmol m^{-2} s^{-1}). A “dynamic threshold” obtained by extracting the best daily threshold values from a range of different simulations helped reduce model overestimation of GPP by 213 g C m^{-2} y^{-1} and reduce RMSE up to 7.7%. Finally, a nonlinear ozone correction based on manipulative experiments produced the best results when no detoxifying threshold was applied (0 nmol O_3 m^{-2} s^{-1}), suggesting that nonlinear functions fully

account for ozone detoxification. The evidence of seasonal changes in ozone tolerance points to the need for seasonal thresholds to predict ozone damage and highlights the importance of performing more species-specific manipulative experiments to derive response functions for a broad range of plant species.

Keywords

Stomatal ozone fluxes, ozone-risk assessment, POD, AIRTREE, Eddy Covariance, GPP.

Introduction

Surface ozone (O_3) is a powerful oxidant of particular concern for plants. O_3 concentrations have doubled in the Northern Hemisphere since the pre-industrial period (annual mean 11-23 ppb) as a result of the release of precursor compounds through industrial activities (Hartmann et al., 2013; Vingarzan, 2004). This secondary pollutant is not directly emitted but formed by sunlight-driven oxidation of other agents, called ozone precursors, like nitrogen oxides (NOx) and volatile organic compounds (VOCs) (Pinto et al., 2010). The Mediterranean climate promotes production of tropospheric O_3 due to sustained photochemical activity driven by dry-hot and sunny summer conditions (Millán et al. 1996; Ochoa-Hueso et al. 2017; Paoletti 2006). O_3 concentrations tend to be elevated in rural areas downwind of big cities which receive plumes of O_3 precursors favoring ozone formation (NIU et al., 2011; Zong et al., 2018). O_3 enters through stomata of leaves where it undergoes oxidation reactions, forming reactive oxygen species and causing damage to biomolecules, including cell membranes, proteins and DNA (Contran and Paoletti, 2007; Fares et al., 2017; Leisner and Ainsworth, 2012; Omasa and Takayama, 2002). This can affect leaf gas exchange and damage the photosynthetic apparatus, leading to plant growth reduction (Paoletti, 2007).

Direct measurement of gas exchange can be performed by the eddy covariance technique (Aubinet et al., 2012). This technique has the advantage that fluxes of a target gas (i.e., CO_2, H_2O or O_3) are recorded at the ecosystem level and are therefore representative of an entire plant community in the footprint of an experimental tower (Fares et al., 2017). Its disadvantages, however, are the lack of direct control over the environmental covariates (i.e. temperature, relative humidity, solar radiation) influencing the ecophysiological processes of the ecosystem and that the measured exchange provides a net flux, which must then be partitioned between stomatal and non-stomatal sources and sinks. Therefore, isolating the stomatal flux of ozone, and its effect on forest ecophysiology, from direct ecosystem-level measurements is challenging especially because the footprint of eddy covariance measurements is representative of all the sources and sinks in the soil-canopy continuum.

Manipulative experiments can be performed in open-top chambers (OTC) or O_3 Free Air Controlled Exposure (O_3-FACE) facilities (Juráň et al., 2021) in order to derive the dose-response functions of a plant's net photosynthesis (*An*) and stomatal conductance (*gs*) to ozone exposure. In order to include the impact of ozone on leaf gas exchange estimates such functions can be coupled to empirical and semi-empirical models of *An* and *gs* such as the widely used Jarvis multiplicative algorithm of stomatal conductance (Jarvis, 1976) and the coupled *A*-*gs* model proposed by Ball, Woodrow and Berry (Ball et al., 1987).

To apply these leaf-level relationships to the ecosystem scale then requires a bottom-up approach. This approach is intrinsic to multi-layer canopy models that combine models of penetration of light with models of leaf-level photosynthesis and models of transport within the canopy to estimate the gas exchange of each canopy layer (Lowman and Rinker, 2004). A variety of multilayer models differing in spatial scale (i.e. local, regional and global model) and time resolution is available. Based on their scope and data availability, different approaches to simulate *gs* and *An* can be used within these models. The canopy gas exchange is generally calculated by integrating the fluxes resulting from various components (i.e. soil, understory, and crown) interacting with their specific microclimate (i.e. profiles of light, humidity and temperature) (Lambers et al., 2019).

Various indices have been developed to evaluate the risks for plants exposed to O_3 (Musselman et al., 2006). The earliest were based on mean atmospheric O_3 concentration (Tong et al., 2009) above a threshold at which damage had been observed in sensitive species. Stomatal uptake of tropospheric ozone is considered a key threat for forest ecosystems (Paoletti, 2007), and specific parameterizations of the stomatal flux of ozone are required to understand the impacts at different sites (Emberson et al. 2000; Mills et al. 2011; CLRTAP 2017).

Inter and intra-species variations in ozone impacts have been observed (Furukawa et al., 1990; Pääkkönen et al., 1996). The nature and magnitude of the response can depend on leaf morphological adaptations, methods for water saving (Feng et al. 2018; Nali et al. 2004; Paoletti 2006) and different strategies of ozone stress resistance such as avoidance of uptake by stomatal narrowing and tolerance to damage in terms of repair and detoxification capacities (Hoshika et al. 2020; Matyssek et al. 2008; Oksanen et al. 2007). Therefore, a better understanding of the flux of O_3 entering through the stomata (i.e. thresholds of detoxification -

phytotoxic dose of ozone (POD_Y) (CLRTAP, 2017)) that leads to the observed O_3 effects on forests and crops stimulates research on ozone-risk assessment.

Based on the premise that new metrics could be evaluated by combining results from manipulative experiments, long-term measurements of O_3, carbon (CO_2) and water (H_2O) fluxes, ancillary measurements and ecophysiological models (Fares et al., 2017), we used the AIRTREE model (Fares et al., 2019) developed to study forest ecosystem services such as carbon sequestration, ozone and particle deposition. AIRTREE uses a coupled *A-gs* sub-model, based on the analytical solution of the Ball-Woodrow-Berry model (hereafter BWB) proposed by Baldocchi (1994) to simulate both gross primary productivity (GPP) and stomatal flux of ozone. Specifically for this study, AIRTREE was implemented with two multiplicative factors for *An* and *gs* as proposed by Lombardozzi et al. (2013, 2015) to improve the predictive ability in simulating the ecophysiological impacts of ozone.

We focused on the Castelporziano eddy covariance forest site in Rome (Italy), for which the AIRTREE model has been calibrated in a previous study (see Fares et al., 2019). The site is characterized by an evergreen Mediterranean Holm oak forest growing in a Mediterranean climate under relatively high ozone concentrations. Using linear and nonlinear responses to ozone exposure derived from species-specific manipulative experiments, four different parameterizations of ozone dose-response relationship were applied in AIRTREE under the assumption that these can provide better model skill than those based on generic formulation for specific PFTs. The goals of this study were to test: 1. which stomatal ozone flux detoxification threshold (POD_Y) best reproduces Holm oak's vulnerability to ozone and if these vary during the season, and 2. if a dynamic function reflecting daily changes in POD_Y can be applied.

1. Materials and Methods

1.1 Study site

The Presidential Estate of Castelporziano, located on the coast of the Tyrrhenian Sea ~25 km from Rome, represents a hotspot for biodiversity in the Mediterranean area, hosting more than 1000 plants species (Davison et al., 2009). It is a protected area of about 4800 ha, of which 85% are forests. The study site, "Grotta di Piastra" (Fluxnet code IT-Cp2 - 10.18140/FLX/1440233; hereafter referred to as CPZ), is located in a wild coastal rear dune ecosystem within the Estate, 1.5 km from the seashore (41°70’42’’N, 12°35’72’’E). The vegetation at CPZ is dominated by an even-aged (49 years) evergreen Holm oak forest (*Quercus ilex* L). The mean height of the forest is 14 m and the average Leaf Area Index (LAI), measured using a portable instrument (mod. LAI 2000, Licor, USA) is 3.00 m^2 leaf m^{-2} ground. The understory vegetation is poorly developed and predominately small mock privet shrubs (*Phillyrea latifolia* L.). The land has a flat topography and the soil is a calcareous Regosoil having a mean depth of 0.45 m, sandy texture and low water-holding capacity. Wind circulation follows a sea-land breeze regime; the dominant wind direction is S-SW during the morning and N-NE during the afternoon. The site is characterized by the typical Mediterranean climate, with pronounced seasonality. Summers are hot and dry, and Winters are moderately cold with mean temperatures of the coldest and warmest months of 7 and 24 °C. Precipitation occurs mostly during Spring and Fall with mean annual precipitation around 700-1100 mm y^{-1}. Here we focus on the year 2013 and 2014, of which, 2013 is considered a moderately dry year with an annual precipitation of 848 mm, while 2014 was wet with an annual precipitation of 1100 mm.

2.2 Meteorological and flux data

A two-year dataset (2013 and 2014) was used to parameterize and evaluate the model. Air temperature, precipitation, relative humidity, net solar radiation, wind direction, soil humidity and soil temperature were recorded every minute and averaged for 30 min intervals with a Davis meteorological station (Davis Instruments Corp. CA, USA, mod. Vantage Pro). Continuous eddy covariance measurements of fluxes from the top of a 21-m scaffold tower started in 2012 and measurements are still ongoing. A tridimensional sonic anemometer (Gill mod. wind master) was used to measure instantaneous wind speed and temperature fluctuations. CO_2 concentrations were measured with an infrared gas analyzer (Licor LI-7200). Air was drawn at 10 l min^{-1} through a 25 m ¼ “ teflon line to an ozone fast analyzer developed by the National Oceanic and Atmospheric Administration (NOAA, Silver Spring, MD) using a chemiluminescence method. The chemiluminescence detector was calibrated against 30 min average ozone concentrations from a factory calibrated UV ozone monitor (Thermo Scientific™ Model 49i). Data were recorded at 10 Hz for all gases using data loggers (CR-3000, Campbell Scientific, Shepshed, UK). In this study GPP was calculated from ecosystem scale fluxes of CO_2 (NEE) by adding the ecosystem respiration term (R_{eco}) to NEE, since NEE represents the balance between CO_2 sequestrated and emitted by the photosynthetic (GPP) and respiratory (R_{eco}) processes of the ecosystem. For more details on the site and meteorology, see Fares et al. (2014) and Conte et al. (2019).

2.3 Leaf-level gas exchange measurements in an O_3 FACE facility

We derived O_3 dose-response functions for *An* and *gs* accordingly to Lombardozzi et al. (2012, 2013) using published leaf gas exchange data for 2 years-old *Q. ilex* seedlings measured in an O3-FACE experiment (Hoshika et al., 2020). The experiment was carried out at the experimental garden of the National Research Council at Sesto Fiorentino (43° 48' 59" N, 11° 12' 01" E), 300 km north from CPZ site. The FACE facility consists of a network of vertical Teflon tubes which fumigate plants with controlled concentrations of O_3. The FACE system was described in detail in Paoletti et al. (2017). Plants were exposed to two levels of ozone concentration (ambient air, AA, as control; 1.4 times ambient ozone concentration, 1.4 × AA) and two levels of water treatments (WW [well-watered]: 100 % field capacity (FC) on average; and WS [water-stressed]: 40% FC on average). There were three replicated plots (Length × Width × Height: 5 m × 5 m × 2 m) in each O_3 treatment (n = 3 replicated plots), with three plants per each combination of O_3 and water. Leaf gas exchange measurements were made by a portable gas analyzer (mod. CIRAS-2, PP Systems, Herts, UK) in a light-saturated condition (photosynthetic active radiation = 1500 µmol m^{-2} s^{-1}) with a constant leaf temperature (25 °C), CO_2 concentration (380 ppm) and air humidity (vapor pressure deficit = 1.0 to 1.8 kPa) during May to September 2015. Other details were described in previous papers (e.g. Hoshika et al., 2020).

2.5 The AIRTREE model

The Aggregated InteRpreTation of the eneRgy balance and water dynamics for Ecosystem sErvices assessment (AIRTREE) model is a multi-layer model that couples soil, plant and atmospheric processes to simulate exchanges of CO_2, H_2O, O_3, and PM between leaves and the atmosphere. A detailed description of the AIRTREE model can be found in Fares et al. (2019, 2020), so here we confine ourselves to a description of the coupled stomatal conductance-photosynthesis parameterization and ozone deposition scheme.

In-situ measurements of solar radiation (PPFD+NIR, Near Infrared Radiation), air temperature, relative humidity, wind speed, CO_2, O_3 and PM concentrations were used to determine the leaf temperature, stomatal conductance, and radiative transfer at five heights from the top to the bottom of the canopy crown. Individual leaf gas exchange is estimated at each layer and integrated to obtain fluxes at the canopy level. The sensible (*H*) and latent (λE) heat fluxes inside each canopy layer from the leaves to the atmosphere are computed as described by Lhomme (1988); see Table S1.

The leaf photosynthetic rate (*An*) was calculated following the Farquhar-von Caemmerer-Berry (FvCB; Farquhar et al., 1980) model as the minimum of the carboxylation rate when ribulose bisphosphate (RuBP) carboxylase/oxygenase is saturated (*Wc*) and when RuBP regeneration is limited by electron transport (*Wj*). This is coupled with the stomatal conductance model of Ball, Woodrow and Berry (the BWB model), and the two are simultaneously solved following the methodology of Baldocchi (1994) to calculate *An* and *gs*. Canopy-scale *An* and *gs* were obtained by integrating values calculated for each layer according to the fraction of sunlight and shaded leaf area.

In-canopy, soil, cuticular, atmospheric and leaf boundary layer resistances to ozone deposition for each layer were calculated as proposed by Zhang et al. (2002). Fluxes of CO_2 (*GPP*), water (λE), and stomatal ozone reported in this study resulted from the integration of each layer contribution.

As soil moisture significantly affects stomatal control, in this study the hydrological sub-model implemented in AIRTREE was deactivated and direct measurements of SWC collected at CPZ were used. The physiological response to drought stress was modelled following Keenan et al. (2010), such that the CO_2 carboxylation rate (*Vc)* is:

$$Vc = Vc_{max} * W_{fac} \qquad \text{eq. 1}$$

where

$$W_{fac} = \begin{cases} 1, & if\ \Theta \geq \Theta max \\ \left[\dfrac{\Theta - \Theta min}{\Theta max - \Theta min}\right]^q, & if \Theta < \Theta max \end{cases} \qquad \text{eq. 2}$$

Vc_{max} *is* maximum CO_2 carboxylation rate, Θ is volumetric soil water content, Θmax is the critical soil water content at which reductions of GPP are first evident and Θmin is the minimum SWC at which GPP was observed (Figure S1). The exponent q is a measure of the non-linearity of the effects of soil water stress on physiological processes (a value of 0.3 was found to best replicate the response at Castelporziano).

2.6 Ecophysiological response to ozone flux

POD is the phytotoxic ozone dose (Emberson et al., 2001), a metric used to standardize plant responses to chronic ozone exposure by integrating ozone flux into the leaf through time. Within the AIRTREE model, POD_Y is calculated using modelled *gs* and the accumulated ozone concentrations during daylight hours, following the approach of Lombardozzi et al (2012):

$$POD_Y = CEO_3 \times g_s \times 1.67 \times 3600 \times 10^{-6} \quad \text{eq. 3}$$

Where CEO_3 is the cumulative ozone exposure above a threshold derived from the manipulative experiment (see Section 2.3) by multiplying the enhanced treatment ozone hourly concentration (1.4*Ambient Air (AA)) for the daily hours of exposure and for the number of days between the start of the exposure and each measurement.

The impact of the stomatal ozone flux, represented by POD_Y, on a plant's ecophysiological processes is simulated in the AIRTREE model by two dose-response factors (Fc_{O3} and Fp_{O3}) representing the response of *An* and *gs*, respectively, to the phytotoxic ozone dose (POD_Y) taken up through the stomata (Lombardozzi et al. 2013 and 2014). The dose-response factors are derived from the regression line fitted to correlations between the treatment to control ratio of *An* and *gs* and the calculated phytotoxic ozone dose POD_0.

The photosynthesis dose-response factor (fp) is calculated as:

$$F_{pO3} = a_p \bullet POD_Y + b_p \quad \text{eq. 4}$$

$$F_{cO3} = a_c \bullet POD_Y + b_c \quad \text{eq. 5}$$

Where a_p and a_c are the slopes and b_p and b_c are the intercepts of the linear regression of *An* and *gs* vs. POD_Y, respectively (see Table 1).

The ozone-impacted photosynthesis and stomatal conductance are then estimated as:

$$An = An \bullet F_{pO3} \quad \text{eq. 6}$$

$$gs = gs \bullet F_{cO3} \quad \text{eq. 7}$$

Critical ozone thresholds are defined in this study as the critical stomatal ozone fluxes above which ozone stress occurred. Consequently, dose-response factors were applied only when stomatal ozone flux was above the selected thresholds.

Four different parameterizations of the dose-response factors were implemented into the AIRTREE model. The first two, represent the linear response function of generic broadleaves characterized by low (BL) and high (BH) vulnerability to ozone, developed by Lombardozzi et al. (2015). The third parameterization (LI) was calculated using the same linear approach (Table 1) from specific dose-response studies on *Quercus ilex* by Alonso et al. (2014) and Fares et al. (2019).

Finally, a fourth parameterization (NI) representing the non-linear response function based on an ad-hoc fumigation experiment on *Quercus ilex* in the O_3-FACE facility was developed. A non-linear regression was fitted to estimates of POD_0 and measurements of *An* and *gs* from doy 148 to 252 (n=10) similarly to Lombardozzi et al. (2013, 2015). The function providing the best fit, based on lowest RMSE (Figure S. 2, S. 3) was used in this study, giving expressions for dose-response factors of:

$$F_{pO3} = 0.998 \bullet e^{(-0.0003 \bullet POD_Y)} \quad \text{eq. 8}$$

$$F_{cO3} = \frac{(0.841 \bullet POD_Y + 31.29)}{(POD_Y + 32.4)} \quad \text{eq. 9}$$

which were applied to *An* and *gs* as in eq. 6-7.

As can be seen from eq. 4 and 5, this method modifies the optimal rates of *An* and *gs* calculated in the model, separating the responses of *gs* and *An* to ozone (Lombardozzi et al., 2015).

With the goal to identify (if one exists) the threshold that best reproduces the Eddy Covariance observations at CPZ, simulations for each model parameterization (BH, BL, LI and NI) were repeated 6 times (for a total of 24 model runs), only changing the critical ozone threshold value (ranging from 0 to 5 nmol m^{-2} s^{-1}) representing high to low sensitivity to ozone, respectively.

Quercus ilex is an evergreen broadleaf forest species with a vegetative period which can last all year long in particularly warm years (Conte et al. 2019). Exposure of leaves to ozone is therefore continuous and the turn-over of leaves, on average, is three years. In order to evaluate if a "memory effect" exists (i.e. the cumulative effects of ozone for more than one year), a value of CEO_3 corresponding to one year of exposure was tested as a starting point; all model simulations were repeated with differing CEO_3 values. Finally, these "memory effect" simulations were compared with simulations with "no memory effect" (i.e. assuming ozone stress starts anew at doy 1).

2.7 Modeling and Statistics

AIRTREE was calibrated for Castelporziano using the 2013-2014 dataset, following the iterative approach explained in detail in Fares et al. (2019). In order to detect and evaluate possible effects of O_3 on the forest's ecophysiological processes (here represented by GPP), data collected when half-hourly O_3 concentration were considered potentially threatening for the vegetation (≥40 ppb) were excluded from the calibration process.

The first model simulation (hereafter named Control) was performed without any ozone effect on A_n and g_s (i.e. with F_{pO3} and F_{cO3} set to unity) and then used as a reference for the other model runs. For each of the four ozone corrections (i.e. BL, BH, LI, NI), six additional model simulations, differing only by the critical ozone dose threshold (hereafter named thr0, thr1, thr2, thr3, thr4, thr5) were run. Model performance was assessed by regression analysis of observed vs simulated GPP. The "best" model run was identified as that which gave the highest coefficient of determination (R^2) and maximum accuracy (lowest RMSE).

Following the approach adopted during model calibration, to avoid double-counting of ozone impacts, we focused on data collected when half-hourly ozone concentration was above 40 ppb, considered the threshold for ozone impacts. To evaluate if the application of the ozone thresholds would have a seasonal positive or negative effect, linear regressions were performed on filtered data for both the whole year and for each season.

Once the best model had been selected, half-hourly values of GPP obtained from each simulation (thr_i) were compared with observations. At each model time step, the simulation with values closer to the observations (*Obs*) was identified and a daily (i.e. n was set to 48 as the number of half-hourly data in one day) threshold variable (*THR*, with values ranging between 0 and 5 nmol O_3 m^{-2} s^{-1}) was finally derived.

$$THR = \frac{1}{n}\sum_{i=1}^{n} min\,|Obs - thr_i| \qquad \text{eq. 10}$$

Pearson's correlation coefficients (r) >0.5 between *THR* and daily mean values of photosynthetically active radiation (PAR), vapour pressure deficit (VPD), soil water content (SWC), air temperature (T_{air}) and ozone concentration (O_3) were arbitrarily used to identify environmental variables which affected *THR*. In order to derive response functions, a boundary line analysis (Gerosa et al., 2009; Webb, 1972) was performed by fitting non-linear regressions to *THR* and the selected variables. We tested six non-linear functions (tables S 6,7) and selected the one providing the best fit with *THR*, based on lowest RMSE. We finally adopted the best function for each variable to develop a Jarvis-like multiplicative algorithm to predict potential THR_p:

$$THR_p = THR_{max} * f_{PAR} * f_{Tair} * f_{VPD} * f_{SWC} * f_{O3} \qquad \text{eq. 11}$$

Where THR_{max} was set at 5 nmol m^{-2} s^{-1} and each function ranged between 0 and 1.

3. Results

3.1 Ozone response intercomparison

In general, incorporating ozone dose-response functions produced a better prediction of GPP for both 2013 and 2014 compared with model simulation when ozone impacts were neglected (Figures 1, S. 4), with low or no differences observed in R-squares and more evident differences observed in the RMSE and slopes of the correlation between model simulations and control.

By applying the BL correction (i.e. the linear correction for generic Broadleaf trees with low vulnerability to ozone), no significant variation in model accuracy was observed among the different thresholds tested for the year 2013. R^2_{adj} remained the same while model accuracy (RMSE) reduced by only 1.2% when a threshold of 1 nmol m^{-2} s^{-1} was applied (Table S. 2). On a seasonal level, when compared to the Control run, for both 2013 and 2014 an improvement in RMSE of ≤3 % was observed in Summer and Fall, when the thresholds of 0 and 1 nmol O_3 m^{-2} s^{-1} were applied (Table S. 2).

By applying the BH response (i.e. the linear correction for generic Broadleaf trees with High vulnerability to ozone) the model accuracy in simulating GPP increased, compared to the Control run, by 2.5% for the year 2013 when a threshold of 1 nmol m^{-2} s^{-1} was applied (Tables S. 3). For 2014, BH corrections increased model accuracy but reduced the slope of the correlation with control values. On a seasonal level the application of ozone corrections during Winter and Spring reduced model accuracy up to 27% in 2013, while a 4% increase in RMSE was observed in Spring 2014 using a threshold of 5 nmol m^{-2} s^{-1}. In Summer and Fall 2013 ozone correction reduced RMSE up to 20 and 11%, respectively, compared to the Control run when a threshold of 1 nmol m^{-2} s^{-1} was applied. In Summer and Fall 2014, the higher thresholds (4-5 nmol m^{-2} s^{-1}) increased model accuracy in simulating GPP.

We found no improvement in simulated GPP when thresholds of 0-1 nmol m^{-2} s^{-1} were applied for either year with the LI function for the entire year in 2013 (i.e. the species-specific linear response function for *Quercus ilex*), while we observed a slight 2 % improvement in RMSE in 2014 when thresholds of 4-5 nmol m^{-2} s^{-1} were applied (Table S. 4). No amelioration from ozone corrections were observed in Winter and Spring 2013, while slight improvements in RMSE were observed in Spring 2014 when thresholds of 4-5 nmol m^{-2} s^{-1} were applied. In Summer 2013, model accuracy in simulating GPP increased up to 28% when a threshold of 1 nmol m^{-2} s^{-1} was applied relative to the Control run, while model predictions in 2014 were all underestimated.

Similarly, the NI species-specific nonlinear response function for *Quercus ilex* did not improve model predictions when applied over the full year 2013 (Table S. 5), except for a slight improvement of model accuracy (RMSE) in simulating GPP by 4.5% relative to the Control run when no tolerance threshold was applied (thr0). In 2014, model correction improved RMSE by up to 4 % at thresholds of 2-5 nmol m^{-2} s^{-1}, although GPP resulted slightly underestimated. More relevant effects of ozone corrections were observed in Summer and Fall 2013, with a model accuracy which increased by up to 9.6 % at thr0 relative to the Control run. In Winter and Spring, no significant increases were observed (R^2_{adj} and RMSE improved by <2%). In 2014, the biggest improvement in simulated GPP was seen in Spring and Fall, with thresholds of 0 and 2 nmol m^{-2} s^{-1}, respectively, increasing model accuracy by up to 8%.

3.2 Dynamic critical ozone threshold

By focusing on cumulative values, deviations (%) between simulated and observed GPP for each season are shown in Figure 2 for both the LI and NI model parameterizations, which were found to be the approaches that produced GPP values closer to observations in our intercomparison. The LI parameterization produced values closer to observations in Summer (below 10% when thr0 and thr1 were applied), and in Fall when thr2, thr3 and thr1 were applied. None of the thresholds resulted in an improvement in model-observation fit in Winter or Spring, with an underestimation of GPP up to 30%.

Similarly, for the NI model we found GPP values closer to observations when thr0 was applied in both Summer and Fall. The application of a critical threshold in Winter and Spring was either ineffective (similar as the Control run) or, in the case of thr0, slightly worsened the model results compared with observations. Of the two approaches, the LI model appeared more dependent on threshold variation among seasons than the NI model, suggesting that plants response varies during the year and that a non-linear model better accounts for the processes underlying the seasonal dependence of the critical ozone threshold.

Such seasonality was evaluated on a daily scale for the LI model (Figure 3). While the daily threshold value (*THR*) showed some correlation with PPFD (r= -0.48 $p<0.05$) and SWC (r= 0.37 $p<0.05$), no correlation was found with O_3 concentration. *THR* values were found to be relatively strong correlated to VPD (r= -0.69 $p<0.05$) and air temperature (r= -0.64 $p<0.05$) and for this reason response functions of *THR* were developed taking into account these two variables only (Figure 4). THR_p was then calculated dynamically within the model as follows:

$$THR_p = THR_{max} * f_{Tair} * f_{VPD}; \qquad \text{eq. 12}$$

where THR_{max} is the maximum threshold for ozone tolerance (5 nmol m^{-2} s^{-1}), f_{Tair} and f_{VPD}, describe the relationships between *THR* and changes in air temperature (°C) and vapor pressure deficit (kPa) as shown in Figure 3.

The response of *THR* to changes in VPD was found to be best described by the Fourier function (Table S. 6):

$$f_{VPD} = 0.56 + 0.40 * cos(x * 1.64) + 0.059 * sin(x * 1.64) \qquad \text{eq. 13}$$

with $R^2 = 0.92$ and RMSE = 0.37,

While the response to air temperature (Table S. 7) was best modelled as:

$$f_{Tair} = (-0.026 * x^2 + 1.45 * x + -6.08) / (x + -3.92) \qquad \text{eq. 14}$$

with R^2 = 0.82 and RMSE = 0.068.

The linear correlation between observed daily threshold *THR* and simulated dynamic threshold derived by the multiplicative model THR_p (eq. 10) is shown in Figure 5 (R^2 =0.5 $p<0.05$). The application of the multiplicative model to LI led to an increase in model accuracy (R^2 increased by up to 5.9% and RMSE reduced up to 7.7%) in simulating GPP (Figure 6) compared to the Control run.

4. Discussion

4.1.1 Ozone dose-response factors

The critical ozone thresholds applied here represent the maximum stomatal ozone flux that a plant is able to tolerate before a toxic dose would start to accumulate. A range of thresholds from 0 (POD0) in the most sensitive species (Musselman et al., 2006) up to 5 nmol m^{-2} s^{-1} in more tolerant PFT have been observed. Lombardozzi et al. (2012, 2015) conducted a series of sensitivity analyses to test the importance of the O_3 threshold value to projected ozone impacts by applying critical values of 0, 0.8, 1.6 and 5 nmol m^{-2} s^{-1} for each PFT in the Community Land Model (CLM) (Lawrence et al., 2012; Oleson et al., 2013). The authors concluded that a threshold of 0.8 nmol m^{-2} s^{-1} could be applied to all PFTs. Sitch et al. (2007), applied thresholds of 1.6 and 5 nmol m^{-2} s^{-1} for woody and grass PFTs in the MOSES-TRIFFID vegetation module of the UK Met Office Unified Model (Cox et al., 1999; Essery et al., 2003). The authors deduced that ozone tolerance in crops varied through the growing period, and the possibility that the same variation occurs in forests is still an open debate (Sitch et al., 2007). Mediterranean evergreen broadleaf tree species are typically considered tolerant to O_3 because of their sclerophyllous leaves, their water saving strategy and ability to tolerate oxidative stress (Hoshika et al. 2020; Nali et al. 2004; Paoletti 2006). Therefore, the Mediterranean climate is a perfect candidate to test the effect of ozone on forests exposed to an oxidative environment.

In this study, four different ozone dose-response functions were evaluated: two PFT-based linear functions (BH and BL) representing broadleaf trees with high and low vulnerability to ozone exposure, respectively; a species-specific linear function (LI) based on field observations of *Quercus ilex* (Fares et al., 2019); and a species-specific non-linear function (NI) based on trials in an O_3 FACE facility. The inter-comparison between PFT-based and species-specific ozone corrections enabled us to evaluate if the well-known ozone tolerance of *Quercus ilex* (Fares et al., 2014, 2019) could be accounted for by standard PFT-based corrections. Unsurprisingly, model performance was substantially better when species-specific parameters were used. Of the three linear approaches used in this study, the *Quercus ilex*-specific LI function outperformed the PFT-based functions by 7% in simulating GPP. In contrast with the previously reported high tolerance of *Quercus ilex* toward oxidative stress (Paoletti, 2006), however, AIRTREE performed better when the high vulnerability (BH) PFT-based formulation was used.

The species-specific ozone dose-response functions derived here from experimental data on *Quercus ilex* provided interesting insights. The lower intercepts (0.79 and 0.86 for A_n and *gs*, respectively) of the regression line between % change from control and ozone-corrected model data translate into a higher correction factor for *gs* than for *An* (Table 1), thus denoting a strong decoupling (about 7%) between the two parameters as previously observed (Fares et al. 2013 GCB; Lombardozzi et al. 2012). At first glance, these results may suggest that *Quercus ilex* is an ozone sensitive species. *Quercus ilex* showed an adaptation strategy with stomatal regulation (avoidance strategy with lower F_{cO3}) to ozone entry in the intercellular spaces. However, the lower values of F_{pO3} suggests that avoidance does not actively prevent this species from ozone damage (Hoshika et al. 2020).

Overall, when different ozone detoxification thresholds were compared, a stomatal ozone flux threshold corresponding to 1 nmol O_3 m^{-2} s^{-1} provided the best results when considered on an annual basis. Similarly, Gerosa et al. (2015) identified thresholds of 1 and 4 nmol m^{-2} s^{-1} for *Quercus ilex* in open top chambers (OTC) experiments when considering total biomass and for roots and leaf biomass, respectively. This result also appears to be in line with the UNECE manual for assessing the impact of ozone on vegetation that suggests the adoption of a threshold for forest vegetation of 1 nmol O_3 m^{-2} s^{-1} (i.e. POD1) (CLRTAP 2017; Mills et al., 2010). However, when assessed on a seasonal basis, the use of an ozone detoxification threshold improved model performance only in Summer and Fall (when ozone concentration is high), with negligible or even deleterious effects when applied in Spring and Winter (Figure 2). This appears to suggest that the detoxifying capacity of *Quercus ilex* changes over the seasons and that a fixed threshold of 1 nmol m^{-2} s^{-1} may not represent the proper metric for this species. Indeed, by focusing on cumulative seasonal values (Figure 2), the use of a fixed threshold for the entire year (i.e. thr1 for each season) introduced in the LI correction seems to play as a compensation factor which attenuates the impact of ozone damage among seasons at least in 2013 (i.e. the real impact should be very moderate in cold seasons and more pronounced in warm seasons). Moreover, the slopes (a_c and a_p) of the linear correction factors (Table 1) are close to 0, leading to a fixed reduction of 21% and 14% for *An* and *gs*, respectively (intercepts). In the wet year 2014, the LI correction did not ameliorate model predictions probably due to a possible overestimation of reducing effect of soil water stress which led to a model underestimation when accounting for ozone effect.

Decoupling the drought effects during warm seasons from ozone effects is a grand challenge which we tried to solve with the use of neural network analysis in a recent work (Savi et al. 2020). However, a low plasticity was described for *Quercus ilex* by Limousin et al. (2010), who found that xylem hydraulic and anatomical properties exhibit a limited plasticity under drought stress. Our findings may suggest that drought alone is unlikely to be responsible for *gs* reduction, but that ozone may play a significant role. The reduction of ozone tolerance in Summer is reasonably explained by the high ozone concentrations combining with high *gs* (Gerosa et al., 2009), with concurrent decrease of the antioxidant defense (Dizengremel et al., 2008). Possible changes in plant's responsiveness to oxidative stress among seasons (Dizengremel et al., 2008; Luwe and Heber, 1995; Sitch et al., 2007) could be accounted for by identifying the proper seasonal thresholds as we show in next section.

4.1.2 Adoption of a dynamic threshold to implement linear approaches

Results of this study suggest that when a linear correction is applied, a fixed threshold may lead to unrealistic estimation of ozone effects on *Quercus ilex* and that a dynamic rather than a fixed threshold may better reflect the actual plant strategies to face ozone stress through the growing season. Significant correlations between daily thresholds (THR) and environmental parameters allowed us to derive a simple empirical model to describe changes in plant sensitivity to ozone due to variation in environmental conditions (i.e. VPD and air temperature) (Figure 3). To simulate these dynamics, a multiplicative empirical approach was tested. Although the weak points of a multiplicative approach are well known (Damour et al., 2010; Tardieu et al., 1996), the choice of an empirical approach for this exercise was driven by data availability and the simplicity of using a formulation based on changes in environmental parameters. THR showed significant correlations with VPD and temperatures (Pearson's r>0.6), but also with soil moisture (0.37) and solar radiation (-0.48). While high radiation and temperatures favor ozone formation (Millán et al., 2000) and a correlation with THR is expected, water availability (SWC) and VPD seem to be more related to the drought stress period typical of the Mediterranean climate, thus suggesting that ozone may exacerbate the effect of oxidative stress due to drought (Alonso et al., 2014; Hoshika et al. 2020).

Relatively low but statistically significant linear correlations (R^2 =0.5) between the observed best daily threshold (*THR*) and the dynamic thresholds estimated by the multiplicative model (THR_p) were obtained. Such a poor fit can be explained by the fact that in this work only six thresholds were used while intermediate values could best represent shifts in ozone tolerance during the day, and that other important variables might not have been included in the analysis (i.e. phenology).

The cumulative values (Figure 6) resulting from the application of the empirical dynamic threshold model (*THR*) provided promising results. Using a dynamic threshold helped reducing model overestimation in comparison with control by 213 g C m^2 y^{-1} for GPP. This translates into simulated cumulative GPP values much closer to observations (with an underestimation of 0.5% compared with observed GPP) than results obtained by applying the best fixed threshold (LI correction at thr1) identified after this iterative approach.

4.2 Performances of non-linear correction factors

A non-linear correction (NI) was estimated from a manipulative fumigation experiment in an ozone FACE facility specifically carried out on *Quercus ilex* saplings of the same genotype of those adult trees at the Castelporziano Estate. As expected, by comparing linear and non-linear approaches, the NI correction resulted to be the best option, increasing model accuracy in simulating GPP for the whole year up to 8.5%. With the application of NI correction, we found the application of either a fixed or dynamic threshold for detoxifying ozone to be unnecessary (i.e. thr_0 provided the best results with NI), suggesting that all the ozone entered into the stomata has an effect but its impact changes during the year by following a nonlinear trend (Fig. S2-S3). When considering the seasonal dynamics of the response to ozone, the non-linear model, similar to LI, showed that ozone correction should not be applied during Winter and Spring, while it provides better estimates in Summer and Fall (Figure 2).

So, we hypothesize that NI accounts for both the tolerance and avoidance strategies, providing the best description of the *Quercus ilex* responsiveness to ozone. A recent study by Agathokleous et al. (2019) supports the hypothesis that an hormetic-like biphasic dose-response function would be more representative of the plant's adaptive responses to ozone exposure, including a compensation phase. This may explain why our nonlinear ozone correction based on species-specific manipulative experiments (NI) provided better results and a detoxification threshold was not necessary.

We would therefore recommend this approach be adopted for modelling the response of all forest ecosystems to ozone exposure. However, in the absence of the necessary species-specific dose-response relationships, a linear response with dynamic threshold based on the multiplicative empirical approach would be the best alternative.

4.3 Is a memory effect relevant?

We hypothesized that a plant's response to ozone might last beyond a season, given that *Quercus ilex* is an evergreen species with a three-year cohort of leaves (Barbeta and Peñuelas, 2016), and it would be reasonable to expect that leaves from previous years could have a different sensitivity to ozone exposure than leaves from the current year (Zhang et al., 2014). The previous simulations were repeated by assuming an additional year of cumulated exposure to ozone (CEO_3), in order to evaluate if the responses to ozone exposure could be affected by a "memory effect" from the previous growing season. Since ozone damage cannot accumulate in BH and BL (slope equal to 0), we applied this hypothesis only to the LI and NI response functions. However, no significant improvements in model performance were observed (not shown), thus indicating that a memory effect is not expected for *Quercus ilex*. Most likely, periods of low ozone concentrations and low stomatal conductance during Fall and Winter allow for full restoration of antioxidant molecules of thick and wax-coated leaves of *Quercus ilex*.

5. Conclusions

A bottom-up integrated model-measurement approach was used to evaluate the effect of ozone exposure on plant ecophysiological processes. By integrating leaf level measurements of gas exchange, manipulative experiments, meteorological data and multi-layer canopy models, this effect was upscaled to the canopy level and compared with *GPP* derived from Eddy Covariance fluxes of carbon. To define a threshold of phytotoxic ozone dose for trees with known ozone sensitivity, we tested four approaches ranging from high to low ozone vulnerability, from PFTs to species-specific responses, from linear to nonlinear approaches. The implementation of ozone dose-response functions into the AIRTREE model improved the accuracy of the simulations of GPP by as much as 8.5% and allowed us to identify which formulation was most appropriate for a Holm oak (*Quercus ilex*) forest growing in a Mediterranean climate, where ozone concentrations are relatively high and seasonal droughts common.

We observed that, as expected, species-specific linear and nonlinear dose-response functions performed better than PFT-based ones. Linear response functions derived for *An* and *gs* revealed that *Quercus ilex* response to ozone exposure is not only driven by stomatal control (avoidance strategy) but also detoxification thresholds play a significant role in describing *Quercus ilex* responsiveness to ozone stress. Such a role may be interpreted as: 1) the plant capacity to produce antioxidants to face oxidative stress induced by ozone entered into stomata (tolerance strategy), or 2) a compensation factor necessary to regulate the impact of ozone corrections for periods during which the oxidative stress may be less relevant (i.e. Winter for the Mediterranean climate).

Recognizing critical stomatal ozone fluxes (i.e. critical ozone thresholds), is crucial for a realistic quantification of its impact on plant ecophysiological processes. Our results, describing plant responsiveness to oxidative stress, identified a critical threshold of 1 nmol m^{-2} s^{-1} (POD1) as the most appropriate for the Holm oak forest when a linear approach was used, thus confirming the guidelines provided by the UNECE manual (CLRTAP 2017; Mills et al. 2010). However, this was not the case when considered on a seasonal rather than annual basis. Differences in the most effective threshold value during different seasons were observed, suggesting that a possible way to implement metrics for ozone-risk assessment could be to derive a dynamic threshold which takes into account possible changes in ozone sensitivity at different time scales during the vegetative period. This is plausible, based on previous work describing different responses to oxidative stress according to the hour of the day and the season (Dizengremel et al., 2008; Luwe and Heber, 1995; Sitch et al., 2007). Changes in ozone tolerance were found to be correlated with environmental parameters that affect ozone formation (temperature and radiation) and plant stomatal regulation (soil moisture and vapour pressure deficit). Therefore, a simple empirical model to predict changes in ozone tolerance was developed for use with the linear response function, providing substantially better model-measurement fit.

In conclusion however, this study suggests that the development of species-specific non-linear ozone dose-response functions represent a key for improving metrics for ozone risk assessment. Since existing literature data does not always allow the derivation of nonlinear functions, new manipulative experiments are highly needed and it is crucial to find a synergy between modelling needs and manipulative experimental design. This synergy would allow the retrieval of useful data (i.e. number of replicates and coherent experimental conditions) to derive reliable dose-response function usable in process models, which would substantially improve our understanding of the impact of ozone on forest ecosystems.

Tables and Figures

Table 1 - *Values used to parameterize plants' sensitivity to ozone (f_c, f_p) by applying a linear approach. Slopes and intercepts are unitless. BL and BH represents the linear corrections for broadleaves characterized by low and high vulnerability to ozone, respectively. LI represents the species specific linear model for Quercus ilex.*

Parameterization	**Slope (ap)**	**Intercept (bp)**	**Slope (ac)**	**Intercept (bc)**	**Reference**
BL	0	0.9798	0	0.9425	Lombardozzi et al., 2015
BH	0	0.8502	0	0.89	Lombardozzi et al., 2015
LI	-0.00027	0.79	-0.0009	0.86	Fares et al., 2019

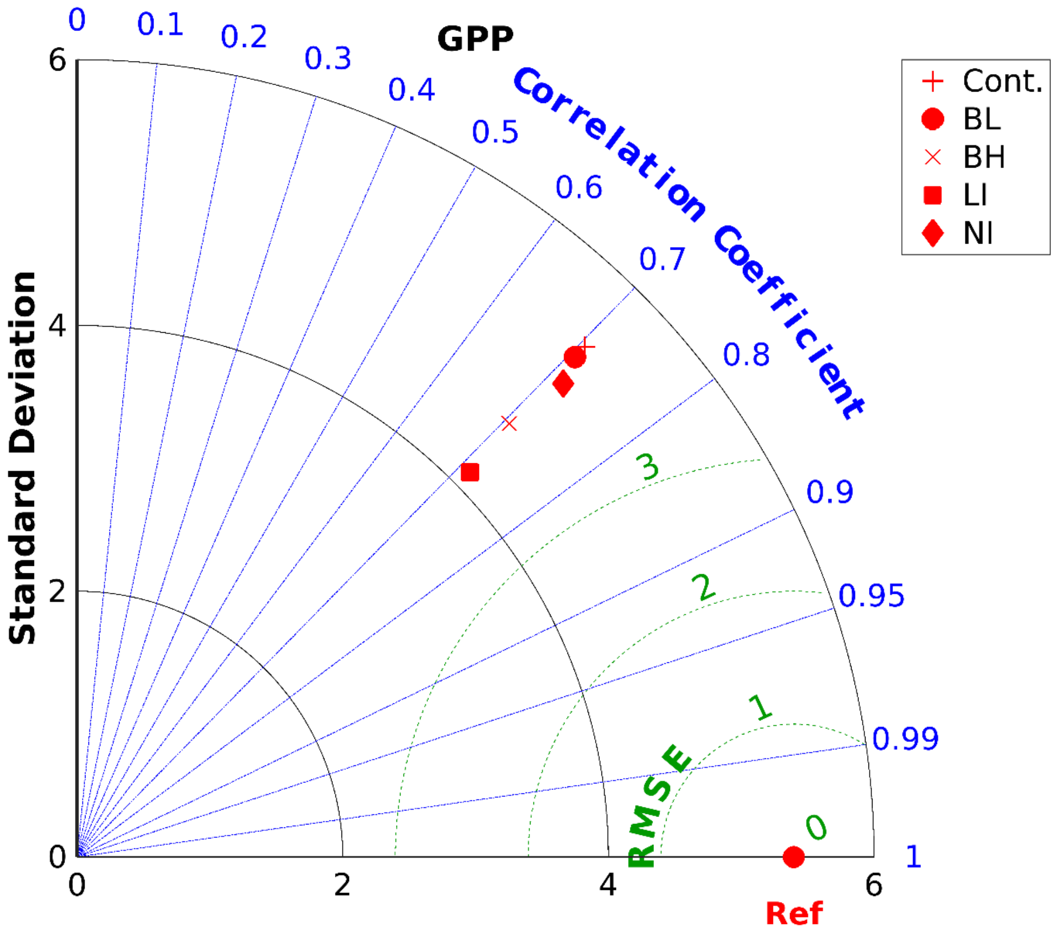

Figure 1: Taylor diagram including statistics on the ozone correction intercomparison. The figure shows the accuracy of the AIRTREE model in simulating GPP for the year 2013. Different symbols represent the performance (Pearson's r, standard deviation and root-mean-square error) of each ozone correction when compared to the observation (Ref). The Control simulation (Cont.) represents a model simulation without any ozone correction. BH and BL are the high and low tolerance parameterization for the broadleaves PFTs suggested by Lombardozzi et al (2015) when a threshold of 1 nmol m^{-2} s^{-1} was applied. LI and NI are the linear and non-linear parameterization of the response of Quercus ilex to ozone when a threshold of 1 and 0 nmol m^{-2} s^{-1} were applied, respectively.

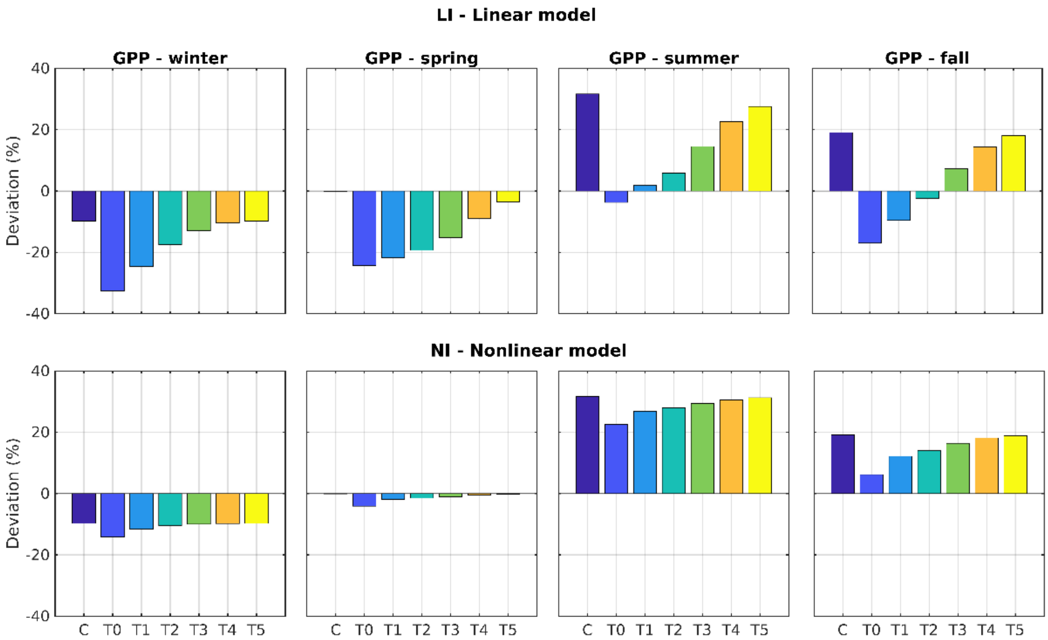

Figure 2: For each season, bars show percent deviation from measured values of Gross Primary Productivity (GPP) using the LI and NI models. Coloured bars refer to increasing critical ozone threshold. Control (C) represents differences between measured and control values when ozone correction was not applied (i.e. negative values mean model underestimation compared with observations). Threshold (T) represents differences between measured and modelled values in response to different levels of ozone tolerance (i.e. thr_i, from 0 to 5 nmol O_3 m^{-2} s^{-1}).

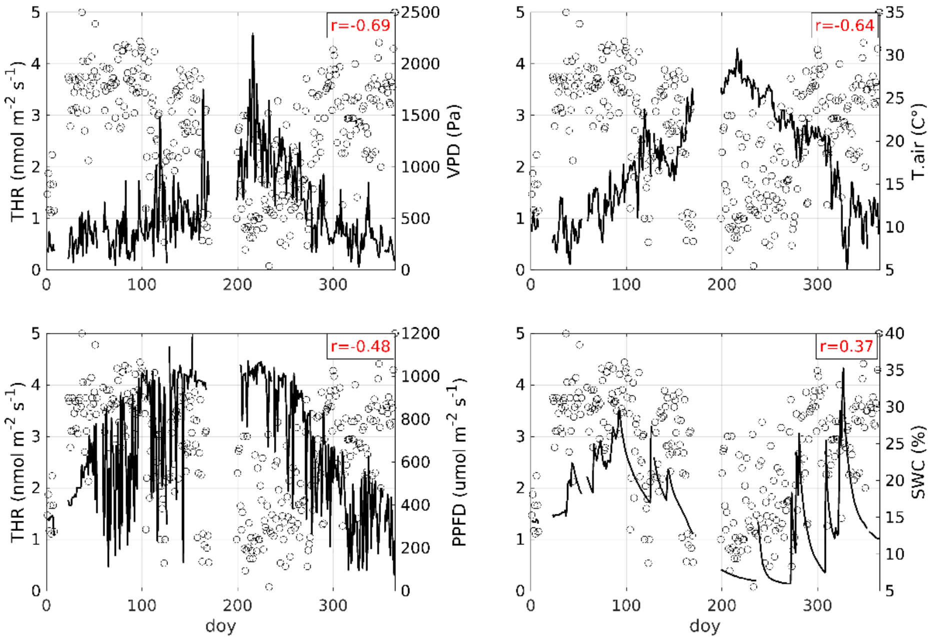

Figure 3: *Pearson's r correlation coefficients (in red) between the best daily threshold THR (empty circles) and the vapor pressure deficit VPD (top left), the Air temperature (Top right), the photosynthetic photon flux density PPFD (bottom left) and soil water content SWC (Bottom right) for Castelporziano site for the year 2013.*

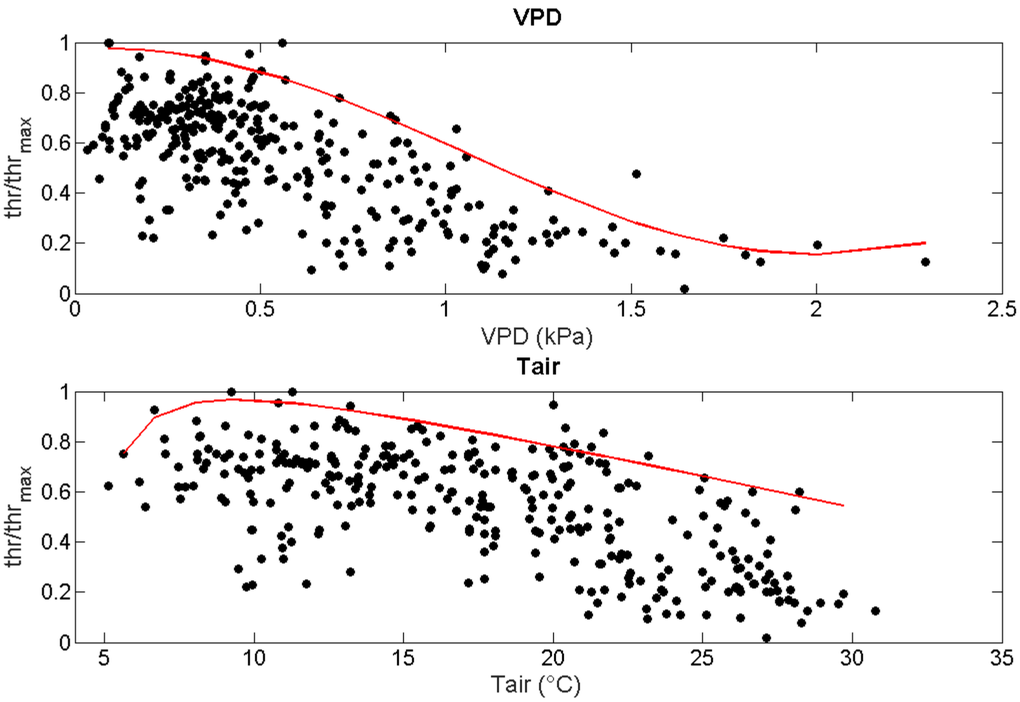

Figure 4: response function of the daily threshold variable (THR) derived by the boundary line analysis to environmental parameters for which significant correlations ($p < 0.05$) were observed. Best non-linear models with goodness of fit is reported in Tables S. 6 and S. 7.

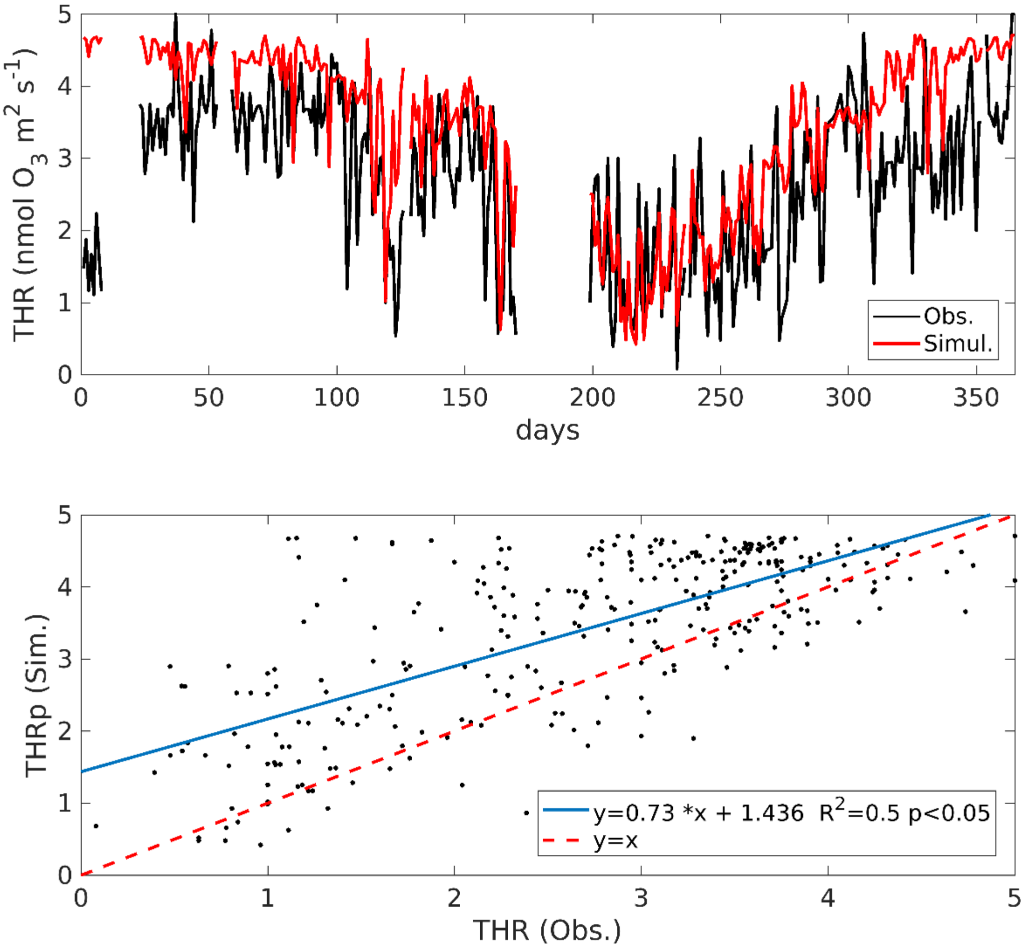

Figure 5: Comparison (top) between the ozone daily threshold THR variable observed (in red) in this study (Ob.) the dynamic threshold model THRp derived (in black) by the multiplicative model. The linear correlation (blue line) between observed THR and simulated THRp is shown on the bottom figure.

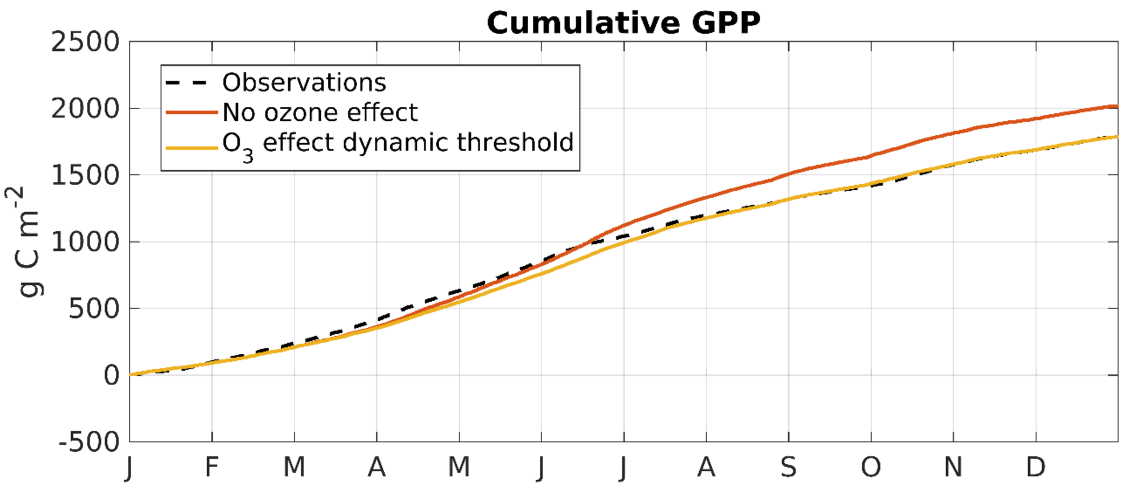

Figure 6: Cumulative values of Gross Primary Productivity (GPP) simulated by applying the dynamic threshold multiplicative correction. The black dashed line represents observations (Obs.). The orange line represents the modelled values without any ozone correction. The yellow line (expected) represents the best modelled values identified by the dynamic threshold at each model time step.

Acknowledgments

The research was made possible thanks to the Scientific Commission of Castelporziano, the Multi-disciplinary Centre for the Study of Coastal Mediterranean Ecosystems and the Directorate of Castelporziano Estate. We want to thank the UE LIFE financial instrument (LIFE18 PRE IT 003) project VEG-GAP "Vegetation for Urban Green Air Quality Plans", the Italian National project PRIN 2017-EUFORICC "Establishing Urban FORest based solutions In Changing Cities", the Regione Lazio project TECNOVERDE: "Tecnologie geomatiche e ambientali di precisione per il monitoraggio e la valorizzazione dei servizi ecosistemici delle infrastrutture verdi urbane e peri-urbane", the Italian National grant CASTEL4 and the Royal Society of London grant DH150070. Thanks also to the Fondazione Cassa di Risparmio Firenze (2013/7956) for supporting the ozone FACE development.

Bibliography

Agathokleous, E., Belz, R.G., Calatayud, V., De Marco, A., Hoshika, Y., Kitao, M., Saitanis, C.J., Sicard, P., Paoletti, E., Calabrese, E.J., 2019. Predicting the effect of ozone on vegetation via linear non-threshold (LNT), threshold and hormetic dose-response models. Sci. Total Environ. 649, 61–74. https://doi.org/10.1016/j.scitotenv.2018.08.264

Alonso, R., Elvira, S., González-Fernández, I., Calvete, H., García-Gómez, H., Bermejo, V., 2014. Drought stress does not protect Quercus ilex L. from ozone effects: Results from a comparative study of two subspecies differing in ozone sensitivity. Plant Biol. 16, 375–384. https://doi.org/10.1111/plb.12073

Aubinet, M., Vesala, T., Papale, D., Kb, D.P.D.F., William, J.M., Loescher, H.W., Luo, H., Rebmann, C., Kolle, O., Heinesch, B., Queck, R., Ibrom, A., Foken, T., Leuning, R., Oncley, S.R., M, M., Aubinet, M., Aubinet, M., Feigenwinter, C., Heinesch, B., Laffineur, Q., Papale, D., 2012. Eddy Covariance: A Practical Guide to Measurement and Data Analysis. p. 460. https://doi.org/10.1007/978-94-007-2351-1

Baldocchi, D., 1994. An analytical solution for coupled leaf photosynthesis and stomatal conductance models. Tree Physiol. 14, 1069–1079. https://doi.org/10.1093/treephys/14.7-8-9.1069

Ball, J.T., Woodrow, I.E., Berry, J.A., 1987. A Model Predicting Stomatal Conductance and its Contribution to the Control of Photosynthesis under Different Environmental Conditions, in: Progress in Photosynthesis Research. Springer Netherlands, Dordrecht, pp. 221–224. https://doi.org/10.1007/978-94-017-0519-6_48

Barbeta, A., Peñuelas, J., 2016. Sequence of plant responses to droughts of different timescales: lessons from holm oak (Quercus ilex) forests. Plant Ecol. Divers. 9, 321–338.

CLRTAP (Convention on Long-Range Transboundary Air Pollution), 2017. Mapping Critical Levels for Vegetation. Man. Methodol. Criteria Model. Mapp. Crit. Loads Levels Air Pollut. Eff. Risks Trends. Chapter 3 Mapp. Crit. levels Veg. 2017, 66.

Conte, A., Fares, S., Salvati, L., Savi, F., Matteucci, G., Mazzenga, F., Spano, D., Sirca, C., Marras, S., Galvagno, M., Cremonese, E., Montagnani, L., 2019. Ecophysiological Responses to Rainfall Variability in Grassland and Forests Along a Latitudinal Gradient in Italy. Front. For. Glob. Chang. 2, 1–12. https://doi.org/10.3389/ffgc.2019.00016

Contran, N., Paoletti, E., 2007. Visible Foliar Injury and Physiological Responses to Ozone in Italian Provenances of Fraxinus excelsior and F. ornus . Sci. World J. 7, 90–97. https://doi.org/10.1100/tsw.2007.10

Cox, P.M., Betts, R.A., Bunton, C.B., Essery, R.L.H., Rowntree, P.R., Smith, J., 1999. The impact of new land surface physics on the GCM simulation of climate and climate sensitivity. Clim. Dyn. 15, 183–203. https://doi.org/10.1007/s003820050276

Damour, G., Simonneau, T., Cochard, H., Urban, L., 2010. An overview of models of stomatal conductance at the leaf level. Plant, Cell Environ. https://doi.org/10.1111/j.1365-3040.2010.02181.x

Davison, B., Taipale, R., Langford, B., Misztal, P., Fares, S., Matteucci, G., Loreto, F., Cape, J.N., Rinne, J., Hewitt, C.N., 2009. Concentrations and fluxes of biogenic volatile organic compounds above a Mediterranean macchia ecosystem in western Italy.

Dizengremel, P., Le Thiec, D., Bagard, M., Jolivet, Y., 2008. Ozone risk assessment for plants: Central role of metabolism-dependent changes in reducing power. Environ. Pollut. 156, 11–15. https://doi.org/10.1016/j.envpol.2007.12.024

Emberson, L.D., Ashmore, M.R., Cambridge, H.M., Simpson, D., Tuovinen, J.-P., 2000. Modelling stomatal ozone flux across Europe. Environ. Pollut. 109, 403–413. https://doi.org/10.1016/S0269-7491(00)00043-9

Emberson, L.D., Ashmore, M.R., Simpson, D., Tuovinen, J.-P., Cambridge, H.M., 2001. Modelling and Mapping Ozone Deposition in Europe. Water. Air. Soil Pollut. 130, 577–582. https://doi.org/10.1023/A:1013851116524

Essery, R.L.H., Best, M.J., Betts, R.A., Cox, P.M., Taylor, C.M., Essery, R.L.H., Best, M.J., Betts, R.A., Cox, P.M., Taylor, C.M., 2003. Explicit Representation of Subgrid Heterogeneity in a GCM Land Surface Scheme. J. Hydrometeorol. 4, 530–543. https://doi.org/10.1175/1525-7541(2003)004<0530:EROSHI>2.0.CO;2

Fares, S., Alivernini, A., Conte, A., Maggi, F., 2019. Ozone and particle fluxes in a Mediterranean forest predicted by the AIRTREE model. Sci. Total Environ. https://doi.org/10.1016/j.scitotenv.2019.05.109

Fares, S., Conte, A., Alivernini, A., Chianucci, F., Grotti, M., Zappitelli, I., Petrella, F., Corona, P., 2020. Testing Removal of Carbon Dioxide, Ozone, and Atmospheric Particles by Urban Parks in Italy. Environ. Sci. Technol. 54, 14910–14922.

https://doi.org/10.1021/acs.est.0c04740

Fares, S., Conte, A., Chabbi, A., 2017. Ozone flux in plant ecosystems: new opportunities for long-term monitoring networks to deliver ozone-risk assessments. Environ. Sci. Pollut. Res. 8240–8248. https://doi.org/10.1007/s11356-017-0352-0

Fares, S., Savi, F., Muller, J., Matteucci, G., Paoletti, E., 2014. Simultaneous measurements of above and below canopy ozone fluxes help partitioning ozone deposition between its various sinks in a Mediterranean Oak Forest. Agric. For. Meteorol. 198–199, 181–191. https://doi.org/10.1016/j.agrformet.2014.08.014

Farquhar, G.D., Caemmerer, S., Berry, J.A., 1980. A biochemical model of photosynthetic CO2 assimilation in leaves of C3 species. Planta 149, 78–90. https://doi.org/10.1007/BF00386231

Furukawa, A., Park, S.Y., Fujinuma, Y., 1990. Hybrid poplar stomata unresponsive to changes in environmental conditions. Trees 4, 191–197. https://doi.org/10.1007/BF00225315

Gerosa, G., Finco, A., Mereu, S., Vitale, M., Manes, F., Denti, A.B., 2009. Comparison of seasonal variations of ozone exposure and fluxes in a Mediterranean Holm oak forest between the exceptionally dry 2003 and the following year. Environ. Pollut. 157, 1737–44. https://doi.org/10.1016/j.envpol.2007.11.025

Gerosa, G., Fusaro, L., Monga, R., Finco, A., Fares, S., Manes, F., Marzuoli, R., 2015. A flux-based assessment of above and below ground biomass of Holm oak (Quercus ilex L.) seedlings after one season of exposure to high ozone concentrations. Atmos. Environ. 113, 41–49. https://doi.org/10.1016/j.atmosenv.2015.04.066

Hartmann, D.L., Tank, A.M.G.K., Rusticucci, M., Alexander, L. V., Brönnimann, S., Charabi, Y.A.R., Dentener, F.J., Dlugokencky, E.J., Easterling, D.R., Kaplan, A., Soden, B.J., Thorne, P.W., Wild, M., Zhai, P., 2013. Observations: Atmosphere and Surface, in: Intergovernmental Panel on Climate Change (Ed.), Climate Change 2013 - The Physical Science Basis. Cambridge University Press, Cambridge, pp. 159–254. https://doi.org/10.1017/CBO9781107415324.008

Hoshika, Y., Fares, S., Pellegrini, E., Conte, A., Paoletti, E., 2020. Water use strategy affects avoidance of ozone stress by stomatal closure in Mediterranean trees—A modelling analysis. Plant Cell Environ. 43, 611–623. https://doi.org/10.1111/pce.13700

Jarvis, P.G., 1976. The Interpretation of the Variations in Leaf Water Potential and Stomatal Conductance Found in Canopies in the Field. Philos. Trans. R. Soc. B Biol. Sci. 273, 593–610. https://doi.org/10.1098/rstb.1976.0035

Juráň, S., Grace, J., Urban, O., 2021. Temporal Changes in Ozone Concentrations and Their Impact on Vegetation. Atmosphere (Basel). 12, 82. https://doi.org/10.3390/atmos12010082

Keenan, T., Sabate, S., Gracia, C., 2010. Soil water stress and coupled photosynthesis-conductance models: Bridging the gap between conflicting reports on the relative roles of stomatal, mesophyll conductance and biochemical limitations to photosynthesis. Agric. For. Meteorol. 150, 443–453. https://doi.org/10.1016/j.agrformet.2010.01.008

Lambers, H., Oliveira, R.S., Lambers, H., Oliveira, R.S., 2019. Growth and Allocation, in: Plant Physiological Ecology. Springer, pp. 385–449. https://doi.org/10.1007/978-3-030-29639-1_10

Lawrence, D.M., Oleson, K.W., Flanner, M.G., Fletcher, C.G., Lawrence, P.J., Levis, S., Swenson, S.C., Bonan, G.B., Lawrence, D.M., Oleson, K.W., Flanner, M.G., Fletcher, C.G., Lawrence, P.J., Levis, S., Swenson, S.C., Bonan, G.B., 2012. The CCSM4 Land Simulation, 1850–2005: Assessment of Surface Climate and New Capabilities. J. Clim. 25, 2240–2260. https://doi.org/10.1175/JCLI-D-11-00103.1

Leisner, C.P., Ainsworth, E.A., 2012. Quantifying the effects of ozone on plant reproductive growth and development. Glob. Chang. Biol. 18, 606–616. https://doi.org/10.1111/j.1365-2486.2011.02535.x

Lhomme, J.P., 1988. Extension of Penman’s formulae to multi-layer models. Boundary-Layer Meteorol. 42, 281–291. https://doi.org/10.1007/BF00121587

Limousin, J.-M., Longepierre, D., Huc, R., Rambal, S., 2010. Change in hydraulic traits of Mediterranean Quercus ilex subjected to long-term throughfall exclusion. Tree Physiol. 30, 1026–1036.

Lombardozzi, D., Levis, S., Bonan, G., Hess, P.G., Sparks, J.P., Lombardozzi, D., Levis, S., Bonan, G., Hess, P.G., Sparks, J.P., 2015. The Influence of Chronic Ozone Exposure on Global Carbon and Water Cycles. J. Clim. 28, 292–305. https://doi.org/10.1175/JCLI-D-

14-00223.1

Lowman, M., Rinker, H.B., 2004. Forest canopies. Elsevier Academic Press.

Luwe, M., Heber, U., 1995. Ozone detoxification in the apoplasm and symplasm of spinach, broad bean and beech leaves at ambient and elevated concentrations of ozone in air. Planta. https://doi.org/10.2307/23383610

Matyssek, R., Sandermann, H., Wieser, G., Booker, F., Cieslik, S., Musselman, R., Ernst, D., 2008. The challenge of making ozone risk assessment for forest trees more mechanistic. Environ. Pollut. https://doi.org/10.1016/j.envpol.2008.04.017

Millán, M., Salvador, R., Mantilla, E., Artnano, B., 1996. Meteorology and photochemical air pollution in Southern Europe: Experimental results from EC research projects. Atmos. Environ. 30, 1909–1924. https://doi.org/10.1016/1352-2310(95)00220-0

Millán, M.M., Mantilla, E., Salvador, R., Carratalá, A., Sanz, M.J., Alonso, L., Gangoiti, G., Navazo, M., Millán, M.M., Mantilla, E., Salvador, R., Carratalá, A., Sanz, M.J., Alonso, L., Gangoiti, G., Navazo, M., 2000. Ozone Cycles in the Western Mediterranean Basin: Interpretation of Monitoring Data in Complex Coastal Terrain. J. Appl. Meteorol. 39, 487–508. https://doi.org/10.1175/1520-0450(2000)039<0487:OCITWM>2.0.CO;2

Mills, G., Pleijel, H., Büker, P., Braun, S., Emberson, L., 2010. Chapter 3: mapping critical levels for vegetation. Mapping manual. Manual on methodologies and criteria for modelling and mapping critical loads and.

Musselman, R.C., Lefohn, A.S., Massman, W.J., Heath, R.L., 2006. A critical review and analysis of the use of exposure- and flux-based ozone indices for predicting vegetation effects. Atmos. Environ. 40, 1869–1888. https://doi.org/10.1016/J.ATMOSENV.2005.10.064

Nali, C., Paoletti, E., Marabottini, R., Della Rocca, G., Lorenzini, G., Paolacci, A.., Ciaffi, M., Badiani, M., 2004. Ecophysiological and biochemical strategies of response to ozone in Mediterranean evergreen broadleaf species. Atmos. Environ. 38, 2247–2257. https://doi.org/10.1016/J.ATMOSENV.2003.11.043

NIU, S., XING, X., ZHANG, Z., XIA, J., ZHOU, X., SONG, B., LI, L., WAN, S., 2011. Water-use efficiency in response to climate change: from leaf to ecosystem in a temperate steppe. Glob. Chang. Biol. 17, 1073–1082. https://doi.org/10.1111/j.1365-

2486.2010.02280.x

Oksanen, E., Kontunen-Soppela, S., Riikonen, J., Peltonen, P., Uddling, J., Vapaavuori, E., 2007. Northern environment predisposes birches to ozone damage. Plant Biol. https://doi.org/10.1055/s-2006-924176

Oleson, K., Lawrence, M., Bonan, B., Drewniak, B., Huang, M., Koven, D., Levis, S., Li, F., Riley, J., Subin, M., Swenson, S., Thornton, E., Bozbiyik, A., Fisher, R., Heald, L., Kluzek, E., Lamarque, J.-F., Lawrence, J., Leung, R., Lipscomb, W., Muszala, P., Ricciuto, M., Sacks, J., Sun, Y., Tang, J., Yang, Z.-L., 2013. Technical description of version 4.5 of the Community Land Model (CLM). https://doi.org/10.5065/D6RR1W7M

Omasa, K., Takayama, K., 2002. Image instrumentation of chlorophyll a fluorescence for diagnosis photosynthetic injury. In “Air Pollution and Plant Biotechnology.”

Pääkkönen, E., Metsärinne, S., Holopainen, T., Kärenlampi, L., 1996. The ozone sensitivity of birch (Betula pendula) in relation to the developmental stage of leaves. New Phytol. 132, 145–154. https://doi.org/10.1111/j.1469-8137.1996.tb04520.x

Paoletti, E., 2007. The effects of ozone on Mediterranen forests. For. - Riv. di Selvic. ed Ecol. For. 4, 478–487. https://doi.org/10.3832/efor0490-0040478

Paoletti, E., 2006. Impact of ozone on Mediterranean forests: A review. Environ. Pollut. 144, 463–474. https://doi.org/10.1016/j.envpol.2005.12.051

Paoletti, E., Materassi, A., Fasano, G., Hoshika, Y., Carriero, G., Silaghi, D., Badea, O., 2017. A new-generation 3D ozone FACE (Free Air Controlled Exposure). Sci. Total Environ. 575, 1407–1414. https://doi.org/10.1016/J.SCITOTENV.2016.09.217

Sitch, S., Cox, P.M., Collins, W.J., Huntingford, C., 2007. Indirect radiative forcing of climate change through ozone effects on the land-carbon sink. Nature 448, 791–794. https://doi.org/10.1038/nature06059

Tardieu, F., Lafarge, T., Simonneau, T.H., 1996. Stomatal control by fed or endogenous xylem ABA in sunflower: interpretation of correlations between leaf water potential and stomatal conductance in anisohydric species. Plant. Cell Environ. 19, 75–84.

Tong, D.Q., Mathur, R., Kang, D., Yu, S., Schere, K.L., Pouliot, G., 2009. Vegetation exposure to ozone over the continental United States: Assessment of exposure indices by the Eta-CMAQ air quality forecast model. Atmos. Environ. 43, 724–733. https://doi.org/10.1016/J.ATMOSENV.2008.09.084

Vingarzan, R., 2004. A review of surface ozone background levels and trends. Atmos. Environ. 38, 3431–3442. https://doi.org/10.1016/j.atmosenv.2004.03.030

Webb, R.A., 1972. Use of the Boundary Line in the analysis of biological data. J. Hortic. Sci. 47, 309–319. https://doi.org/10.1080/00221589.1972.11514472

Zhang, L., Brook, J.R., Vet, R., 2002. On ozone dry deposition—with emphasis on non-stomatal uptake and wet canopies. Atmos. Environ. 36, 4787–4799. https://doi.org/10.1016/S1352-2310(02)00567-8

Zhang, W., Feng, Z., Wang, X., Niu, J., 2014. Elevated ozone negatively affects photosynthesis of current-year leaves but not previous-year leaves in evergreen Cyclobalanopsis glauca seedlings. Environ. Pollut. 184, 676–681.

Zong, R., Yang, X., Wen, L., Xu, C., Zhu, Y., Chen, T., Yao, L., Wang, L., Zhang, J., Yang, L., Wang, X., Shao, M., Zhu, T., Xue, L., Wang, W., 2018. Strong ozone production at a rural site in theNorth China Plain: Mixed effects of urban plumesand biogenic emissions. J. Environ. Sci. 71, 261–270. https://doi.org/10.1016/J.JES.2018.05.003